EFDA–JET–CP(07)04/09

E. de la Luna and JET EFDA contributors

Physics of ECE Temperature Measurements and Prospects for ITER

Physics of ECE Temperature Measurements and Prospects for ITER

E. de la Luna and JET EFDA contributors*

JET-EFDA, Culham Science Centre, OX14 3DB, Abingdon, UK

[1]Asociación EURATOM-CIEMAT, CIEMAT, Madrid, Spain
** See annex of M.L. Watkins et al, "Overview of JET Results ",*
(Proc. 21 st IAEA Fusion Energy Conference, Chengdu, China (2006)).

Preprint of Paper to be submitted for publication in Proceedings of the
Inernational Workshop on Burning Plasma Diagnostics, Villa Monastero,Varenna, Italy.
(24th September 2007 - 28th September 2007)

ABSTRACT.
The physics of the Electron Cyclotron Emission (ECE) temperature measurements is reviewed. The current understanding of the expected ECE spectra in ITER is summarized, for perpendicular as well as oblique propagation. The relevance of the use of oblique ECE for investigating the shape of the electron distribution function at low energies is discussed.

1. INTRODUCTION

The capabilities of Electron Cyclotron Emission (ECE) for electron temperature (T_e) measurements have been used for over four decades of magnetic fusion research. In this period the ECE diagnostics have evolved from proof-of-principle experiments [1] to becoming routinely available on all major fusion devices. In addition to the traditional time- and space- resolved electron temperature profile measurements, ECE diagnostics are employed for a wide variety of measurements in the plasma. This includes core MHD localization, perturbative transport experiments, real time control of ITBs and NTMs and electron distribution function measurements [2]. The good spatial and temporal resolution achieved with the available state-of-the-art multichannel radiometers has been a key feature in most of the measurements mentioned above. Moreover, ECE measurements have proved to be a rich source of new and, in some cases, puzzling phenomena, stimulating the development of more specific and ingenious diagnostic applications, such as oblique ECE [3] or sophisticated systems for 2D imaging [4].

However, as magnetic fusion experiments progress toward larger physical dimensions, higher temperatures and densities, the measurement of electron temperatures from the ECE radiated power becomes more challenging. The purpose of this tutorial paper is to review the physics of evaluating T_e from ECE measurements (for other applications see [5] and references therein) and the prospects for the ECE diagnostics in ITER as it is seen from the perspective of today's experiments. The discussion will be primarily focused on the physical interpretation of the measurements rather than on the technical aspects of their implementation [6]. A few examples of experimental data from JET (the closer fusion device to ITER parameters) are used to illustrate the limitations that the ECE diagnostics will encounter when applied to ITER. The main characteristics of the expected ECE spectra in ITER have been discussed in previous Varenna workshops [7][8]. In this paper we extend these earlier results by including the analysis of the emission using different observation angles with respect to the magnetic field.

2. BASICS OF THE ECE THEORY

The source of the cyclotron emission is radiation from the orbital motion of the electrons along the magnetic field lines. A single electron of speed v radiates in an infinite set of harmonics s of the electron cyclotron angular frequency $\omega_{ce} = eB/m_e$, where B is the magnetic field and m_e is the electron rest mass, giving $f_{ce} = \omega_{ce}/2\pi \approx 28$ GHz/T. The polarization of the emitted wave depends on the direction of observation, relative to the magnetic field. For perpendicular observation, the

radiant energy propagates in two characteristic modes called the eXtraordinary or X-mode and the Ordinary or O-mode, characterized by the direction of the wave electric field perpendicular or parallel to the confining magnetic field, respectively.

To calculate the observed emission spectrum two steps are required. The first step involves the evaluation of the emission (b) and absorption (a) coefficients [9]:

$$\beta(\omega, N_{//}) \propto \sum_{s=-\infty}^{+\infty} \int \frac{du^3}{\gamma} \; \delta(\gamma - s\omega_{ce}/\omega - N_{//}\mu_{//}) \; | Pol |^2 f(u) \tag{1}$$

$$\alpha(\omega, N_{//}) \propto \sum_{s=-\infty}^{+\infty} \int \frac{du}{\gamma} \delta(\gamma - s\omega_{ce}/\omega - N_{//}\mu_{//}) \; | Pol |^2 \left[\frac{s\omega_{ce}}{\omega} \frac{1}{u_\perp} \frac{\partial}{\partial u_\perp} + N_{//} \frac{\partial}{\partial u_{//}} \right] f(u) \tag{2}$$

where $\vec{u} = \gamma\vec{v}/c$ is the normalized relativistic momentum, $N_{//} = k_{//}\, c/\omega$ is the parallel component of the refractive index ($k_{//}$ is the component of the wave vector parallel to the magnetic field and c is the speed of light), $\gamma = (1 - v^2/c^2)^{-1/2}$ is the relativistic factor, $|Pol|^2$ is a weighting function that depends on the polarization and the harmonic number, $f(u)$ is the electron distribution function and the subscripts $\|$ and $\perp$ refer to the parallel and perpendicular components with respect to the magnetic field. From these simplified expressions some general properties can be learned:

- The δ- function in the integrals of (1-2) implies that only electrons that satisfy the resonant condition:

$$\omega = \frac{s\omega_{ce}}{\gamma} - k_{//} v_{//} \tag{3}$$

  can contribute to the emission and absorption processes. At each harmonic, three effects will lead to variation of the emission frequency: the radial variation of the magnetic field that changes the cyclotron frequency, a frequency shift due to the relativistic mass which lowers the emission frequency as the energy of the resonant electrons increases ($\gamma m_e c^2$) and the Doppler shift caused by the relative motion between the emitting electrons and the observer.
- The energy and pitch-angle dependence of the weighting function $|Pol|^2$ is different for the two different polarization modes and/or for the different harmonics (for a more detailed description see [9]).

In the second step, the radiation transport equation [10] is solved in order to determine how much of the emitted radiation emerges outside the plasma:

$$\frac{dI(\omega)}{dl} = \beta - \alpha I(\omega) \tag{4}$$

where $I(\omega)$ is the specific intensity at a frequency ω and l is the spatial coordinate along the ray trajectory (the ray refractive index is approximated by unity). Eq. (4) takes into account that part of the emitted radiation is absorbed as the wave propagates through the plasma toward the detection

system. For the specific case of observation from the Low-Field Side (LFS) of the plasma, the solution of Eq. (4) is of the form:

$$I(\omega, N_{//}) = I_{in}(\omega, N_{//}) \exp(-\tau_{12}(\omega, N_{//})) + \int_{l_1}^{l_2} \beta(l, \omega, N_{//}) \exp(-\tau(l, \omega, N_{//}))dl \qquad (5)$$

where $l_1 \le l \le l_2$, being l_1 and l_2 the initial and final points of the ray within the plasma boundaries, the exponential function in the integral is the transmission coefficient and t is the optical depth defined by:

$$\tau(l, \omega, N_{//}) \equiv \int_{l}^{l_2} \alpha(l', \omega, N_{//})dl' \qquad (6)$$

The first term in Eq. (5), which can formally be written as $I_{in}(\omega, N_{//}) = R_w I(\omega, N_{//})$, is the radiation that is reflected off the inner wall of the tokamak and/or the cut-offs, being $\tau_{12}(\omega, N_{//}) \equiv \int_{l_1}^{l_2} \alpha(l, \omega, N_{//})\, dl$ the total optical depth along the path that the ray followed in the plasma. Note that reflections generally also imply significant polarization scrambling and this effect is also included in R_w ($\le$1).

In the case of a plasma in local thermodynamic equilibrium at a local temperature T_e, the emission and absorption coefficients are not independent but related by Kirchhoff's law, their ratio equal to the blackbody radiation, which in the classical limit of the Plank's law can be written as:

$$\frac{\beta(\omega, N_{//})}{\alpha(\omega, N_{//})} = \frac{\omega^2}{8\pi^3 c^2} T_e \qquad (7)$$

Substituting (7) into (5), the radiation temperature $T_{rad}(\omega, N_{//}) = (8\pi^3 c^2/\omega^2)\, I(\omega, N_{//})$ can be conveniently written as:

$$T_{rad}(\omega, N_{//}) \approx \langle T_e \rangle \times \frac{1 - \exp(-\tau(l, \omega, N_{//}))}{[1 - R_w \exp(-\tau_{12}(\omega, N_{//}))]} \qquad (8)$$

where

$$\langle T_e \rangle = \frac{\int_{l_1}^{l_2} T_e(l)\, G(1, \omega, N_{//})dl}{\int_{l_1}^{l_2} G(l, \omega, N_{//})dl} \qquad (9)$$

and

$$G(l, \omega, N_{//}) = \alpha(l, \omega, N_{//}) \times \exp(-\tau(l, \omega, N_{//})) \qquad (10)$$

defines the emitting region, with $\langle T_e \rangle$ being the average temperature within the emitting volume. This factor $G(l, \omega, N_{//})$ has a nearly Gaussian profile and its width is determined by the reabsorption, as described by the transmission factor in Eq.(10). When the reabsorption is large, $\tau \gg 1$ (optically thick plasma), the emitting region is a narrow zone close to the resonance position and the emitted

radiation is a measure of the local T_e (see Fig.1). Note that for optically thick harmonics T_{rad} is independent of wall reflections.

A couple of comments are in order. First, the spatial localization of the emission discussed above is valid when there is only one harmonic contributing to the emitted radiation at a given frequency. Second, the observed emission is not only localized in real space (along the line of sight) but also in velocity space ($u_{//}$,$u_{\perp}$). The correlation between the energy and location of the resonant electrons has immediate physical consequences for the interpretation of the ECE measurements. Let us consider first observation perpendicular to the magnetic field from the low-field side, which is the most common set-up for temperature measurements. For $N_{//} = 0$ the resonance condition is reduced to $\omega = s\omega_{ce}/\gamma$, consequently only electrons with $s\omega_{ce}/\omega > 1$ can contribute to the emission. Because in toroidal fusion devices the magnetic field decreases monotonously along the major radius, the emission at a given frequency is not only originated near the resonance but also from locations in the plasma with higher B and therefore generated by electrons with higher energy ($E = m_e c^2(\gamma - 1) = mec^2(s\omega_{ce}/\omega - 1)$). This emission is often called downshifted emission. To complete the picture we need to include the absorption along the propagation path. Since the absorption depends on the number of resonant electrons, when the distribution function is Maxwell-like, that is when the electron population decreases monotonically with increasing energy ($f(\mathrm{E}) \propto \exp(-E/T_e)$), the low-energy electrons near $\omega \approx \omega_{ce}$ reabsorb the emission coming from the energetic electrons located further inside the plasma ($\omega > s\omega_{ce}$) and, as a result, the radiation that reaches the antenna comes from relatively low energy electrons ($E < T_e$) and is well localized in real space (see Fig.1(a)).

3. OBLIQUE ECE

We now consider the case of oblique observation, i.e. $N_{//} \neq 0$ with $N_{//} < 1$. In this case the resonant condition for oblique observation can only be fulfilled by electrons that satisfy:

$$[s\omega_{ce}(l)/\omega)^2 - 1 + N_{//}(l)^2] > 0 \qquad (11)$$

Eq. (11) sets an outer radial limit on where emission at a given frequency can be originated, while the inner limit of the emitting region is set by the reabsorption. The optical depth decreases with $|N_{//}|$; however for hot and large plasmas, the optical depth of the thermal resonance is sufficiently high to reabsorb the emission coming from $\omega > s\omega_{ce}$ and only a thin layer contributes to the observed intensity (see Fig.1(b)) [11][12]. This emission is often called upshifted, because it comes from a region located to the right of the resonance location. In this scenario the emission from an optically thick harmonic is originated by electrons with energies near or slightly above the thermal energy, $E \geq T_e$ (the energy increasing with increasing observation angle).

The main interest of measuring the emission at different angle to the magnetic field lies in the fact that by changing the observation angle, it is possible to change the range of energies at which

the temperature of the distribution function can be probed. Moreover, the sign of the $N_{//}$ selects the sign of $u_{//}$, which makes the oblique view sensitive to asymmetries in the distribution function.

4. DIAGNOSTIC POTENTIAL OF ECE MEASUREMENTS

The spatial localization of the optically thick harmonics forms the basis of the ECE temperature measurements. Since the cyclotron frequency is determined by the magnetic field and the magnetic field in toroidal devices varies across the plasma in a known way, essentially inversely proportional to the major radius, the location of the origin of the emitted radiation at a given frequency is known and its intensity gives the local temperature at that location. Hence, for optically thick harmonics, the width and shape of the ECE spectrum corresponds to the width and shape of the T_e profile. The optical thickness depends on the plasma parameters (n_e, T_e), the magnetic field gradient, the harmonic number, polarization mode and the angle θ between the viewing direction and the magnetic field ($N_{//} = cos\theta$). For fixed magnetic field gradient and $N_{//}$, the emitting region broadens with increasing T_e and decreasing n_e [13]. The overall radial resolution must be evaluated by taking into account the width of the emission layer, the finite bandwidth of the measurements and the antenna pattern. The first harmonic O-mode (designated by the notation 1O-mode) and the second harmonic X-mode (2X) have the larger optical thickness (with $\tau_{2X} > \tau_{1O}$) and are the most commonly used in present experiments. The condition of $\tau \gg 1$ is not necessary fulfilled at the plasma edge (optically thin plasma), which imposes a limit on how close to the last closed flux surface (R_{LCFS}) reliable T_e measurements can be obtained (see Fig.2). In addition, edge measurements are strongly affected by the presence of small populations of suprathermal electrons. In this case, the unique correspondence between the emitting frequency and the spatial (and energy) location of the emission is lost and the measured intensity is not necessarily related to the local temperature.

Another important issue for the use of ECE diagnostics is the accessibility. The major radius range over which T_e measurements can be made using ECE diagnostics is limited by cut-off effects and harmonic overlap. The use of 2X-mode, which has twice the cutoff density of the 1O-mode, allows for a large range of accessible densities. Since, for 2X-mode measurements, $n_{e,cutoff} \propto B^2$, the cut-off represents no limitation in the operating density for high magnetic field tokamaks like ITER. The 1O-mode, being closer to its cut-off frequency than the 2X-mode, is more susceptible to refraction effects if $\omega_{ce}/\omega_{pe} \rightarrow 1$ (where ω_{pe} is the plasma frequency). Harmonic overlap occurs in small aspect ratio devices because of the large variation in toroidal magnetic field across the plasma, which allows two or more harmonics to resonate at the same frequency in different parts of the plasma. In JET, 3rd harmonic emission near the edge on the low-field side occurs at the same frequency as 2nd harmonic emission from radii inboard of the plasma center. However this limitation does not exist for the 1O-mode. The possibility of using the 1O-mode emission to access the High-Field Side (HFS) of the plasma has been recently explored in JET and simultaneous temperature measurements of the inboard and outboard pedestal region have been obtained [15]. These measurements are particularly relevant for investigating ELM dynamics, specially considering how

poorly diagnosed the plasma in the inboard region is in large fusion devices due to the difficult access for diagnostics.

5. ECE MEASUREMENTS IN HIGH T_e PLASMAS

In the last years, ECE measurements in high T_e plasmas show features that appear to fall outside the standard description. In JET, an apparent disagreement between the central temperature measured by ECE (2X-mode) and Thomson Scattering (TS) have been observed in strong auxiliary heated (NBI+ICRH) plasmas, with ECE showing higher temperature values (up to 15% in cases where T_{e0} >7 keV) in a narrow central region (r/a < 0.35) [16]. Similar discrepancy was reported in TFTR [17] and has remained unexplained so far.

From a formal point of view, agreement between the TS and ECE temperatures occurs only if the electron distribution function is Maxwellian. The peculiarity of the discrepancy observed in JET is that it appears in a region where the plasma is optically thick, which implies that the deviation of the electron distribution function from the Maxwellian must be localized at low energies (if this is the cause of the discrepancy). Since 2nd harmonic ECE and TS measurements carry information on bulk electrons of different energy, discrepancies between ECE and TS temperature profiles can be considered as a proof of the existence of non-Maxwellian features in the bulk electron distribution function (if calibration errors are ruled out). Moreover, ECE spectra measured in those plasma conditions are also inconsistent with the electron bulk distribution being Maxwellian in the plasma core [18]: the central temperature deduced from the 3rd harmonic is lower than the one deduced from the 2X-mode. The 3rd harmonic emission is optically thick in these high temperature plasmas and therefore provides an independent measurement of the bulk electron temperature but related to electrons with higher energy [19]. Similar features in the ECE spectra has been reported in FTU [20] and DIII-D [21] during high power on-axis ECRH experiments. All of these experimental results appear to be consistent with the existence of a distortion in the bulk of the electron distribution function [12]. The detailed understanding of the origin of this intriguing experimental result is crucial when considering the application of the ECE techniques in ITER, where the temperature range over which the temperature measurements are expected will be significantly higher than those of existing tokamaks. Further work to identify the experimental conditions leading to the appearance of the described inconsistency between different T_e measurements in JET is ongoing.

As discussed in the previous section, an attractive and independent method to assess the existence of non-Maxwellian bulk electron distribution functions is oblique ECE. A diagnostic of this kind has been recently installed in JET [3]. This instrument allows the simultaneous measurement of the ECE spectrum at different angles ($\approx 10^o$, $\approx 20^o$) and with different polarizations (O- and X-mode). From the emitted spectra at different observation angles it will be possible to explore the distribution function in a wider energy range. For optically thick harmonics, there exist several frequencies for which on average, the emitting electrons are in the same position but have different energy, which, in principle, could permit an spatially resolved reconstruction of the distribution function.

6. ECE IN ITER

In the high-temperature (> 20keV) plasmas predicted for ITER, the optical depth for the higher harmonics will increase considerably and the level and shape of the ECE spectra will be substantially different from that of the existing tokamaks. In the discussion that follows only thermal plasmas will be discussed. For the effect of suprathermal electron tails on the ECE spectra for ITER see [22]. Previous studies [7][8] have shown that access over a significant portion of the plasma cross-section can be obtained with the 1O-mode (with spatial resolution of 10-15cm), while the use of the 2X-mode, more strongly affected by harmonic overlap, is restricted to the outboard plasma region. On the other hand, the best spatial resolution at the edge (4-6cm) is achieved with the 2Xmode, although the stringent spatial resolution requirements for the edge measurements (5mm) set by ITER can not be met [23].

Let us now examine the case of oblique emission. Shown in Fig.3 are the ECE spectra for $\theta = 0^o$ (perpendicular observation) and $\theta = 10^o$ for parameters typical of the Scenario 2 in ITER along with the corresponding $T_e(f)$ profiles as obtained from $T_e(f = f_{ce})$. Those spectra have been calculated using the emission code SPECE [23].

The main observations are the following:

- $T_{rad}(f) < T_e(f)$ on the high frequency side of the 2X-mode. This can be understood by considering that the 2X-mode emission when propagating toward the antenna in the low field side is reabsorbed by the relativistically downshifted 3X-mode emission (even though the resonance radius for the 3rd harmonic is outside the plasma), being the observed radiation the 3X-mode contribution from the edge outboard plasma region (see Fig.3(c)).
- $T_{rad}(f) > T_e(f)$ on the high frequency side of the 1O-mode. At the plasma edge, the observed intensity is dominated by the downshifted 2O-mode emission (from the high energy tail of the Maxwellian distribution) (see Fig.3(d)).
- $T_{rad}(f) > T_e(f)$ in the lower frequency region for both modes. The optical thickness at the plasma edge is not high enough to reabsorb the downshifted emission from the Maxwellian tail of the hot core plasma.
- core T_e measurements for which $T_{rad}(f)$ matches up the corresponding T_e profile can be obtained from the 1O- and 2O-mode, although the spatial resolution of the 2O-mode is poorer (by more than a factor of 2) than that of the 1O-mode. The same applies to the oblique emission, being the size of the emitting region for the oblique view comparable to that of normal emission [23] (see Fig.3(e)). Note also that the shift in the effective position of the emitted radiation generated by the relativistic broadening, and the Doppler effect in the case of the oblique spectrum, is higher for the 2O-mode.

These results are of course profile dependent. The central region affected by harmonic overlap becomes wider for higher T_e or flatter profiles [7]. As for the impact of the antenna pattern on the overall spatial resolution, the effect of the beam size is negligible for perpendicular observation

(for antennas located on the plasma midplane), whereas it tends to be significant for the oblique observation due to the Doppler effect [23].

CONCLUSIONS

The properties of the ECE radiation in hot plasmas and its potential for measuring the T_e profiles in ITER have been reviewed. We have shown that, for T_e < 30keV, core temperature measurements can be obtained from the 1O- and 2O-mode ECE for both normal and oblique observation (for q < 20^o). Despite the different spatial resolution of the measurements (the spatial resolution worsening with increasing observation angle and harmonic number), having more than one measurements of the central temperature in ITER may be useful as a general consistency check. Furthermore, since those measurements carry information on different regions in velocity space, their comparison would enable to detect distortions on the bulk of the distribution function.

The observed anomaly on the ECE spectra and the apparent discrepancies between the central T_e measured by ECE and TS in high-T_e plasmas seem to indicate that the assumption of a Maxwellian bulk may not be necessarily true in the present of strong auxiliary heating, contrary to what is usually assumed. Based on these experimental findings, we may speculate that non-Maxwellian bulk distribution functions could appear in plasmas with high level of auxiliary power whenever a sufficient amount of the heating power is absorbed by the bulk electrons. However, the extrapolation of these results to ITER remains uncertain because of the lack of a valid physical model for the origin of such a distortion in the distribution function. More experimental and theoretical work is necessary to assess the potential implications of a non-Maxwellian bulk for temperature measurements in ITER.

One point that has been stressed throughout the paper is the fundamental role played by the coupling between the energy and location of the resonant electrons in the evaluation of the T_e from ECE measurements. One intrinsic limitation of the diagnostic is that the information obtained with the ECE measurements can only be related to a narrow region in velocity space, which is determined by both the resonance condition and the reabsorption along the propagation path. In general, it is assumed that the plasma is Maxwellian and, therefore, the distribution function is well described with a single temperature value. However, this will not be the case when the distribution function deviates from the Maxwellian. In such cases, electron population with different energies will have different average temperature, the temperature ceases to be a useful parameter and a description of the velocity distribution is needed. While the appearance of distortions in the ECE spectra is often sufficient to identify the non-Maxwellian features in the distribution function, the problem of inferring quantitative information on the electron distribution function from the shape of the ECE spectra is by no means straightforward. This is an ill-posed problem and does no have a unique solution. The typical approach is to choose an arbitrary distribution function with variable parameters and then, in a quantitative comparison between experiments and theory, these parameters are adjusted for a best fit between calculation and measurement. The accuracy of this procedure can be significantly

improved by using as many independent measurements of the ECE spectrum (at different polarization, harmonics and observation angles) as possible.

ACKNOWLEDGMENTS

The author would like to thank D. Farina, L. Figini and C. Sozzi for providing the ITER spectra presented here. The author also wishes to thank V. Krivenski for giving information, criticism and suggestions on the subject of the oblique ECE. It is not the objective of this paper to give a complete overview of the current activities in the field, therefore there is no attempt to provide exhaustive references and I apologize to those whose work I have unwittingly overlooked.

REFERENCES

[1]. A. Costley et al., Phys. Rev. Letters **33** 758-761 (1974)

[2]. H. Gasparino, Proc. 8th Joint Workshop on ECE and ECRH, Gut-Ising, Germany (1993) pp. 19-44

[3]. C. Sozzi, et al, in this Proceedings

[4]. H.K. Park et al., Phys. Rev. Letters **96** 195004 (2006)

[5]. H.J. Hartfuss Plasma Phys. Control. Fusion **40** A231-A250 (1998)

[6]. H.J. Hartfuss, T. Geist and M. Hirsch, Plasma Phys. Control. Fusion **39** 1693-1769 (1997)

[7]. D.V. Barlett, in Diagnostics for Experimental Thermonuclear Reactors, edited by P. Stott, G. Gorini and E. Sindoni, Plenum Press, New York (1996) pp. 183-193

[8]. D.V. Barlett and H. Bindslev, in Diagnostics for Experimental Thermonuclear Reactors, edited by P. Stott, G. Gorini and E. Sindoni, Plenum Press, New York (1998) pp. 171-180

[9]. M. Bornatici, R. Cano, O. de Barbieri, F. Engelmann, Nuclear Fusion **23** 1153 (1983)

[10]. G. Bekefi, Radiation Processes in Plasmas, Wiley, New York (1966)

[11]. V. Tribaldos and V. Krivenski, Proc. 8th Joint Workshop on ECE and ECRH, Gut-Ising, Germany (1993) pp. 123-141

[12]. V. Krivenski, Fusion Engineering and Design **53** 23 (2001)

[13]. V. Tribaldos, "Spatial Resolution for Electron Cyclotron Emission in JET", JET-Report, EFDA JETPR(01)44 (2001)

[14]. A. G. Peeters et al, Proc. of the 10th JointWorkshop on ECE and ECRH, Ameland, Holland (1997), pp. 403

[15]. L. Barrera, in this Proceedings

[16]. E. de la Luna et al., Review Sci. Instrum.**74** 1414 (2003)

[17]. G. Taylor et al., Proc. 8th JointWorkshop on ECE and ECRH, Gut-Ising, Germany (1993) pp. 277-288

[18]. V. Krivenski, E. de la Luna and G. Giruzzi, Proc. 19th Conference on Controlled Fusion and Plasma Physics, Montreaux (2002)

[19]. I. Fidone, G. Giruzzi and G. Taylor, Phys. Plasmas **3** 2331 (1996)

[20]. G. Bracco et al., Proc. 18th IAEA Fusion Energy Conference, Sorrento, Italy (2000)
[21]. R.W. Harvey et al., Proc. 13th JointWorkshop on ECE and ECRH, Nizhny Novgorod, Russia (2004) pp. 119
[22]. M. Bornatici and U. Ruffina, Plasma Phys. Control. Fusion **38** 1561 (1996)
[23]. D. Farina, L. Figini, P. Platania and C. Sozzi. in this Proceedings

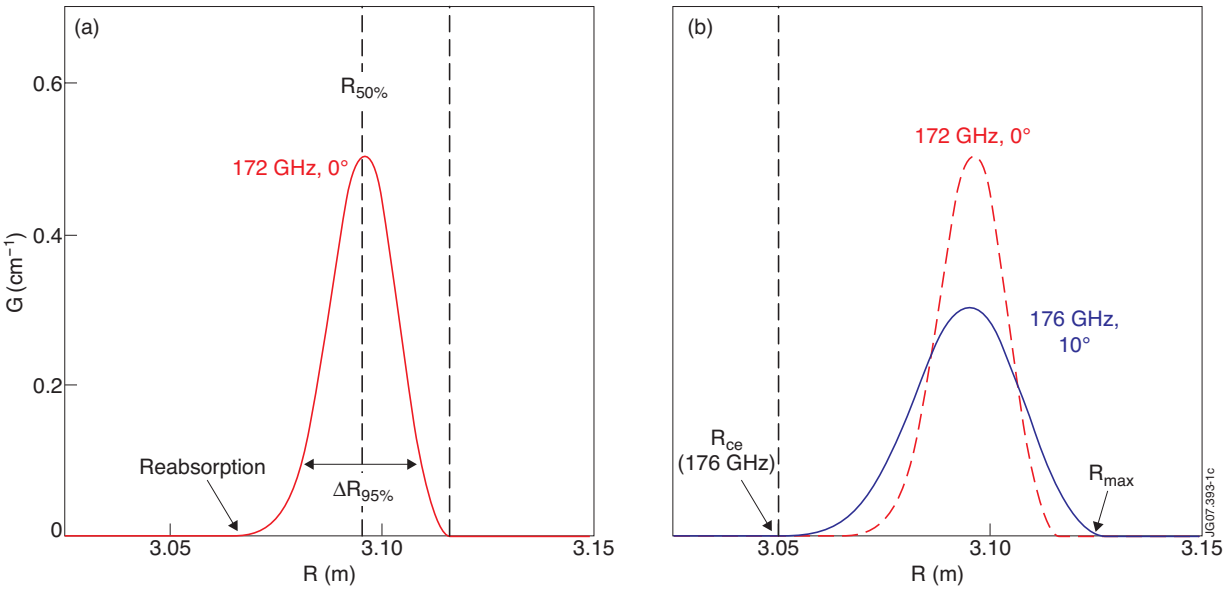

Figure 1: The function G(ω, R) (Eq. 10), determining the size of the emitting region, is shown for two observation angles: a) $\theta = 0^o$ and b) $\theta = 10^o$ for JET plasma parameters (T_{e0} = 7keV, $n_{e0} = 3.5\times10^{19}$ m^{-3}, B= 3.2T). For $\theta = 0^o$ the emission comes from a thin layer on the left of the resonance position R_{ce} whose width is determined by the reabsorption, while for the oblique observation the electrons responsible of the observed radiation are located in a region $R_{ce} < R < R_{max}$, where R_{max} is defined by Eq. (11). The location of the emission is given by the center of gravity of the function G(w, R) and the effective resolution by the radial extension of the region responsible for 95% ($\Delta R_{95\%}$) of the observed intensity.

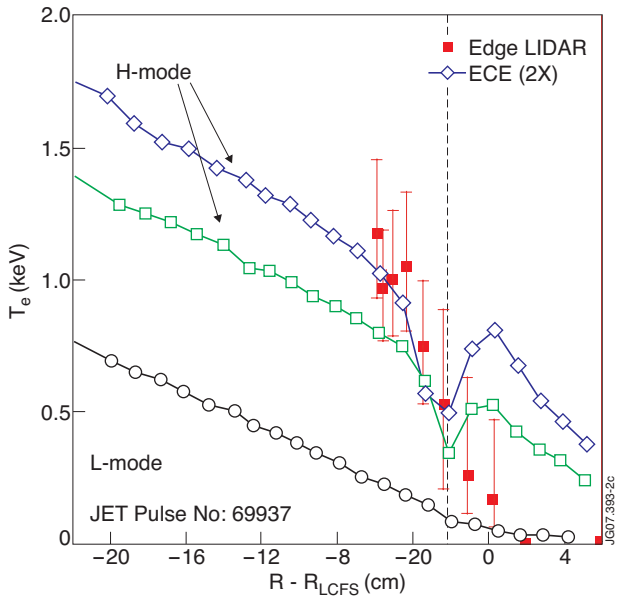

Figure 2: Edge T_e profiles, as measured by ECE (open symbols) and the edge LIDAR system (closed symbols) in JET, showing an enhancement of the T_{rad} (above the corresponding blackbody emission) measured by ECE close to the separatrix during H-mode (this effect is discussed in more detailed in [14])

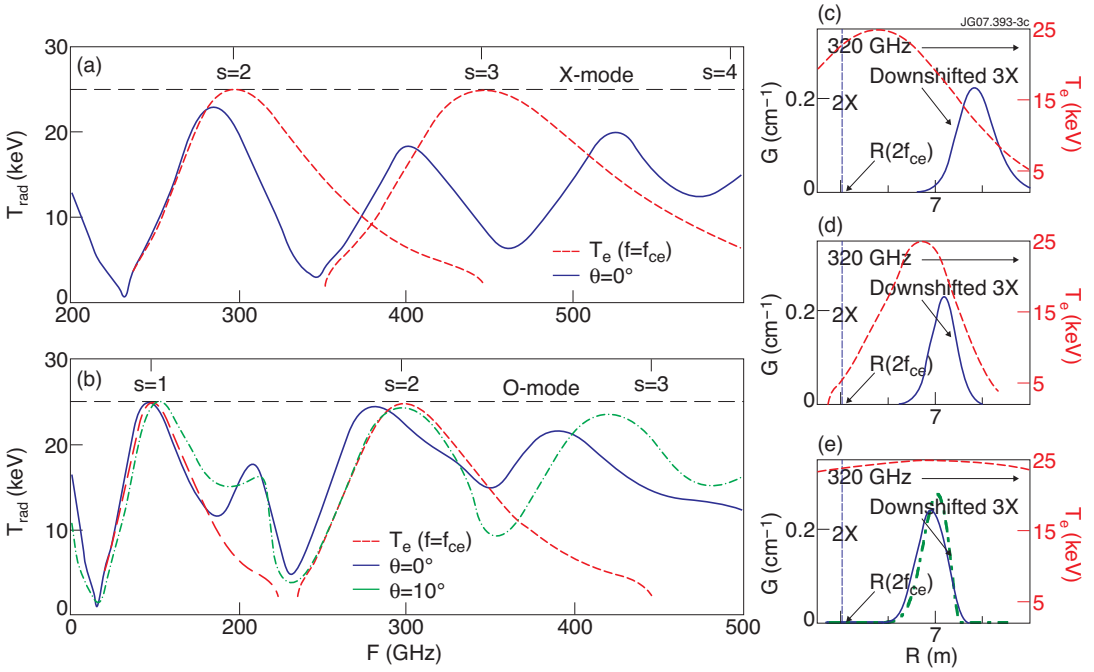

Figure 3: T_{rad} versus $f = \omega/2\pi$ for (a) X-mode and (b) O-mode in ITER (T_{e0} = 25 keV, $n_{e0} = 10^{19}$ m^{-3}, B_0 = 5.4 T) for $\theta = 0^o$ and $\theta = 10^o$ in the case of O-mode and G(R, ω) factor for specific frequencies: (c) X-mode, f = 320GHz, (d) O-mode, f = 204GHz, and (e) two frequencies corresponding to emission from the plasma center for two different observation angles. The thin dashed lines are $T_e(R_{ce})$ versus $f = f_{ce}$.